Multiscale regularization based on turbulent kinetic energy decay for PIV estimations with high spatial resolution

P. Héas[1]**, D. Heitz**[2,3,1] **and E. Mémin**[1]

[1]INRIA, Centre de Recherche de Rennes - Bretagne Atlantique, Campus de Beaulieu, F-35042 Rennes Cedex, FRANCE.

[2]Cemagref, UR TERE, F-35044 Rennes Cedex, FRANCE.

[3]Université européenne de Bretagne, Rennes, FRANCE.
dominique.heitz@cemagref.fr

ABSTRACT

We propose a new multiscale PIV method based on turbulent kinetic energy decay. The technique is based on scaling power laws describing the statistical structure of turbulence. A spatial regularization constraints the solution to behave through scales as a self similar process via second-order structure function and a given power law. The real parameters of the power-law, corresponding to the distribution of the turbulent kinetic energy decay, are estimated from a simple hot-wire measurement. The method is assessed in a turbulent wake flow and grid turbulence through comparisons with HWA measurements and other PIV approaches. Results indicate that the present method is superior because it accounts for the whole dynamic range involved in the flows.

1. INTRODUCTION

The measurement of the displacement field between two images consists in resolving the matching problem between both images, and can be divided into local and global approaches. Local approaches computes the disparity of a given element by observing only its close neighborhood. These region based approaches estimate the similarity at a spatial location by comparing a window around it in the first image with similar windows in the second image, for a given matching cost. Standards costs are cross-correlation and the square of the displaced frame difference. The former is currently used in particle image velocimetry (PIV), while the later is commonly used in computer vision to estimate the optical flow. These techniques are based on disjoint local estimation, need contrasted images and produce sparse vector fields. Since they are robust to noise they remain very popular in industrial community. In contrast, global approaches solve an optimization problem on the entire image, by making global smoothness assumptions. Generally devised in a variational framework, they involve more sophisticated energy optimization methods and provide dense (one vector per pixel) vector fields with spatial coherence. Several spatial regularization have been used. The first-order regularization proposed in the standard optical-flow approach of Horn and Schunk [5] was designed for quasi-rigid motions. Recently, Corpetti *et al.* [1] devised a second-order regularization scheme more adapted for fluid motion since it enforces regions of homogeneous vorticity and divergence. Nevertheless, these high-order spatial-regularization schemes appeared to suffer from a lack of physical consistency with the structure of turbulence and fail to represent precisely the variety of spatial structures particularly at small scales. In addition, since these regularizations do not rely on any fluid mechanics models they need to be weighted by a parameter which has to be tuned for optimal performance.

The purpose of this work is to provide a multi-scale regularizer based on turbulent kinetic energy decay. In contrast to standard approaches, the prior is physically sound and presents the valuable advantage of solving the badly posed problem while fixing regularizers weights at the different scales. The proposed approach consists in constraining the velocity fields, through the second order structure function, to follow the statistical scaling laws as predicted by Kolmogorov [2]. The real parameters of the power-law, corresponding to the distribution of the turbulent kinetic energy decay, were estimated from a simple hot-wire measurement.

This article is organized as follows. In a first section, we present the modeling of turbulence energy decay. Then, in a second section, we present the model-based PIV technique including the multiscla self-similar regularization. In a last part, results from real images in grid turbulence and in the wake of a circular cylinder, are presented and analyzed. We provide some elements of comparison of our method with standard model-based and correlation PIV techniques.

2. MODELING TURBULENCE ENERGY DECAY

The approach of Kolmogorov [2] allows, with simple arguments, the prediction of the turbulence energy spectrum. The non-equilibrium turbulence statistic proposed by Kolmogorov is based on the kinetic enrergy cascade towards small scales. Let us consider the longitudinal velocity structure functions $S_p(\ell) \equiv\, <\delta v(\ell)^p>$, which are the pth order moments of the longitudinal velocity increments $\delta v(\mathbf{x}, \ell\mathbf{n}, t) \equiv (\mathbf{v}(\mathbf{x} + \ell\mathbf{n}, t) - \mathbf{v}(\mathbf{x}, t)).\mathbf{n}$, where $\mathbf{n}$ is unit vector pointing in the direction of ℓ the separation vector between two points.

Under the assumptions that the statistic of $\delta v(l)$ is homgeneous, stationary and isotropic, Kolmogorov proposed that the velocity structure functions have power law dependance on ℓ in the inertial subrange

$$S_p(\ell) \sim \beta\ell^{\zeta_p}, \qquad (1)$$

where the scaling exponent ζ_p was suggested to be equal to $p/3$, indicating a universal behaviour of small-scale fluctuations. The theory of Kolmogorov is based on two assumptions. The first hypothesis of similarity states that for scales ℓ smaller than the integral scale L, the distributions of $\delta v(\ell)$ are universal, and are fixed by the molecular viscosity ν and the mean energy dissipation rate ε. The second hypothesis of similarity for scales ℓ larger than η, the elementary scale of the energy cascade, the distributions of the velocity increments $\delta v(\ell)$ are not dependant of the viscosity ν. Hence, for $\eta < \ell < L$ one has the following

approximation $S_2(\ell) \sim C_2(\varepsilon\ell)^{2/3}$ and $S_3(\ell) \sim C_3\varepsilon\ell$, where C_2 and C_3 are constants. However, due to intermittency effects the scaling exponent ζ_p has in reality a nonlinear dependance on p and non-strict self-similarity is assumed for turbulent flows (Frisch [2]). Nevertheless, for $p = 3$ no deviations of the scaling exponent are expected. Furthermore, any two- or three-dimensional turbulent flow is regular in the dissipative range $0 < \ell < \eta$ and using Taylor expansion the second order structure function reads $S_p(\ell) \sim \beta\ell^2$.

3. METHOD

The proposed method is a model-based measurement technique which belongs to global variational approaches. This PIV technique minimizes an energy functional composed of two terms:

$$f(I,\mathbf{v}) = f_d(I,\mathbf{v}) + \alpha f_r(\mathbf{v}). \quad (2)$$

The image observation model $f_d(I,\mathbf{v})$, also called data term, relates the luminance in the image with $\mathbf{v}$ the velocity field to estimate. Since this first term is not self-sufficient to estimate the two components of velocity in the image plane, a second term $f_r(\mathbf{v})$ is added. This regularization term enforces a global spatial coherence, via spatial dependencies imposed over the whole image domain, to a degree specified by the parameter α weighting the two terms.

3.1 Image observation model

In a recent paper Liu & Shen [7] have described the relation between fluid flow and optical flow. The projected motion equations for several typical flow visualizations have been carefully derived, based on projection of the transport or continuity equation in three dimensions onto the image plane. A generic physic-based data term has been proposed. They have demonstrated that the so called integrated continuity equation model from Corpetti [1], is well suited for laser-sheet illuminated particle and scalar images. Using the phase number equation for particulate flow and the scalar transport equation, they showed that the optical flow is proportional to the path averaged velocity of particles or scalar across the laser sheet and proposed the following physics-based optical flow equation,

$$\frac{\partial I}{\partial t} + \nabla I \cdot \mathbf{v} + I\mathrm{div}\mathbf{v} = g(\mathbf{x},I), \quad (3)$$

$$g(\mathbf{x},I) = D\nabla^2 I + DcB + c\mathbf{n}.(N\mathbf{u})|_{\Gamma_-}^{\Gamma_+},$$

where D is a diffusion coefficient, c is a coefficient for particle scattering/absorption or scalar absorption, $B = -\mathbf{n}.\nabla\psi|_{\Gamma_-}^{\Gamma_+} - \nabla.(\psi|_{\Gamma_-}\nabla\Gamma_- + \psi|_{\Gamma_+}\nabla\Gamma_+)$ is a boundary term that is related to the considered quantity ψ, and its derivatives coupled with the derivatives of the control surfaces Γ_-, Γ_+ of the laser sheet illuminated volume. Since the control surfaces are planar, there is no particle diffusion by molecular process, and the rate of accumulation of the particle in laser sheet illuminated volume is neglected, the term $g(\mathbf{x},I) \simeq 0$.

Discretizing in time the physics-based equation 3 the data term reads,

$$f_d(I,\mathbf{v}) = \frac{1}{2}\int_\Omega (\tilde{I} - I + \nabla I \cdot \mathbf{v} + I\mathrm{div}\,\mathbf{v})^2 d\mathbf{s} \quad (4)$$

where $\tilde{I}$ denotes the image $I(t + \Delta t)$ and Ω is the image domain. For bi-dimensional flows this observation term leads to the classical optical flow constraint equation which is relevant for many geophysical applications as meteorology and oceanography.

Nevertheless, the observation model remains underconstrained, as it provides only one equation for two unknowns (u,v) at each spatio-temporal location $(\mathbf{x},t)$.

3.2 Standard regularization

The first-order regularization proposed by Horn & Schunck [5] is not adapted to fluid flow since it penalizes the vorticity and the divergence. Corpetti *et al.* [1] proposed a second-order regularization minimizing the gradient of the divergence and of the vorticity which reads,

$$f_r(\mathbf{v}) = \frac{1}{2}\int_\Omega (||\nabla\mathrm{div}\mathbf{v}||^2 + ||\nabla\mathrm{curl}\mathbf{v}||^2)d\mathbf{s}. \quad (5)$$

Improvements of this fluid-dedicated regularization have been suggested with precise numerical scheme by Yuan *et al.*[8] or with physics-based spatio-temporal scheme by Heitz *et al.*[4]. However the accuracy of these approaches depend on the tuning of the weighting parameter α.

3.3 Self-similar regularization

The self-similar regularization introduced by Héas *et al.* [3] is a multiscale physics-based model which is not weighted by any subjective regularization parameter. The term is based on the turbulent energy decay power-laws proposed by Kolmogorov (see §2). More precisely the second-order structure function has been used since it provides a convenient quadratic constraint. The new self-similar regularization term defined at each scale ℓ as the difference between the 2-nd order structure function and a given power law reads,

$$f_{r_\ell}(\mathbf{v}) = \frac{1}{2}(S_2(\ell) - \beta\ell^{\zeta_2}) = 0. \quad (6)$$

As indicated in section 2 the second-order structure function does not provide an exact prediction of scaling laws for non-strictly self similar flows. However, in the present study we estimate directly the parameters (β,ζ) from a hot-wire anemometry measurement. Another method proposed by Héas *et al.* [3] would consists in taking into account the deviations from the predicted law by selecting the most likely scaling law defined by parameters (β,ζ) given the image data. $S_2(\ell)$ is an expectation which is obtained by spatial integration over the image domain and over all directions.

3.4 Optimization problem

The minimization problem reads,

$$\begin{cases} \min_\mathbf{v} f_d(I,\mathbf{v}), \ \mathbf{v}(\mathbf{x}) \in \mathbf{R}, \\ \text{subject to the constraints:} \\ f_{r_\ell}(\mathbf{v}) = 0, \ \forall\ell \in \mathbf{I}, \end{cases} \quad (7)$$

where $\mathbf{I}$ is the scale range of the given power law. This system is optimally solved by taking advantage of lagrangian duality. It results in a collection of first-order regularizers acting at different scales. It should be noted that the optimal regularization parameters at the different scales are obtained by solving the dual problem (for more details see Héas *et al.* [3]).

4. EXPERIMENTAL SET-UP

The multiscale approach was evaluated with particle image sequences recorded in one of the wind tunnels of the Rennes regional Center of the Cemagref. These sequences show grid turbulence and the near wake flow of a circular cylinder at Reynolds number Re = 3900.

A square-mesh biplane grid was used to generate approximately homogeneous and isotropic turbulence (see [6]). The grid was mounted at the inlet of testing zone and had a mesh size of 7 mm with diameter d of the bars of 2 mm. The solidity of the grid $\sigma \equiv d/M(2-d/M)$, was 0.49 and the mean velocity U was set at 6 m/s leading to a Reynolds number $Re = UM/\nu$ of 2700.

A circular cylinder was used to generate a turbulent wake flow. the cylinder had a length L of 100 mm and a diameter D of 10 mm. The distance between the ceiling and the floor of the testing zone was 100 mm providing an aspect ratio L/D of 10. The blockage ratio was 10%. The circular cylinder was mounted horizontally and vertically at $3.5D$ from the entrance of the testing zone. The free-stream velocity was adjusted at 6 m/s, giving a Reynolds number of 3900.

2D2C PIV experiments were carried out with a LaVision commercial system including a NewWave laser Solo 3 Nd-YAG (Energy by pulse of 50mJ) and a PCO cameras SensiCam (CCD size of 1280×1024 pixels, pixel size of 6.7×6.7 μm^2 and dynamics of 12bits). A lens with focal length of 50 mm and aperture of 5.6 was mounted on the camera. The magnification factor M was about 14.7 pixels/mm. The field of view was 87.5mm $\times$ 69.9mm, i.e. about $12.5M \times 10M$ or about $8.8D \times 7D$. On average, the particle diameter on the image was of 3 pixels. The images were acquired at the mid-span of the testing zone, i.e. for $z = L/2$, x being in the streamwise direction and y in the vertical direction.

The correlation-based velocity fields were calculated with the commercial software DaVis 7.2 from LaVision. A multipass algorithm with a final interrogation window size of 16×16 pixels and 50% overlapping was applied. Image deformation and round Gaussian weighting function were used. Spurious velocities were identified with median filter, each vector component is checked independently and replaced by the median.

Hot-wire measurements (HWA) were performed with a X-wire probe, providing the longitudinal and the transverse velocity fluctuations. Both wires had a diameter of 2.5 μm and a length of 1 mm inclined at about $\pm 45^o$ relative to the mean flow. The wires were operated with constant temperature at an overheat ratio of 0.8. The signals were sampled at a frequency of 50kHz and digitised with a 16 bit A/D converter. A specific method was developed for the calibration procedure and the signal processing of the X-wire. To have a total calibration time less than ten minutes, we chose to calibrate the probe in a non stationary process by working on continuously varying velocity and temperature conditions, and 16 discrete angle positions ($\pm 38^o$ with 5° increments) in order to determine in a single calibration run all the sensitivities of the measurement system to velocity, temperature and angle. The calibration procedure take into account the the real geometry of the probe, the interaction of the wires, the influence of the temperature and the deviations from King's law at low velocities, the four-dimensional hypersurface for each wire was modelled with 4th-order polynomial equations.

The use of the Taylor's frozen-flow hypothesis allows for direct comparison between HWA and PIV measurements. This assumption is warranted in grid turbulence since the mean velocity is much greater than the turbulent velocity. For the wake flow the validity of the Taylor's hypothesis will be discussed in section 5.

5. RESULTS

The images were acquired with tiny time delay between frames in order to limit the loss of particles due to the out of plane component. This yielded mean longitudinal particle displacements of 1 for the grid turbulence and 1.7 pixels for the wake flow, corresponding to time delays of $5\mu s$ and $10\mu s$, respectively. These particular experimental conditions are optimized for model-based measurement techniques, since limited loss of particles pairs and small displacements better suit the image observation model (equation 4). Indeed, the models are formulated in a variational framework and hence valid for displacements smaller than the smallest wave length in the image (after de-noising). It should be noted that to deal with outliers, like the loss of particle pairs, the data term is equipped with robust penalty functions which indirectly give larger weight to the regularization term [1].

The self-similar regularization was applied on the first two length scales in the image domain, i.e. for separations from one to two pixels. This range belonged to the dissipative range $0 < \ell < \eta$, since the Kolmogorov dissipation length scale η, estimated with HWA, was 0.23 mm or 3.3 pixels for grid turbulence and 0.13 mm or 1.8 pixels for the wake flow. Hence for the regularization term we used the second-order structure function $S_p(\ell) = \beta \ell^2$. The parameter β was estimated with HWA measurements. As a consequence, through the used of β the solution is constrained with the real rate of energy transfer.
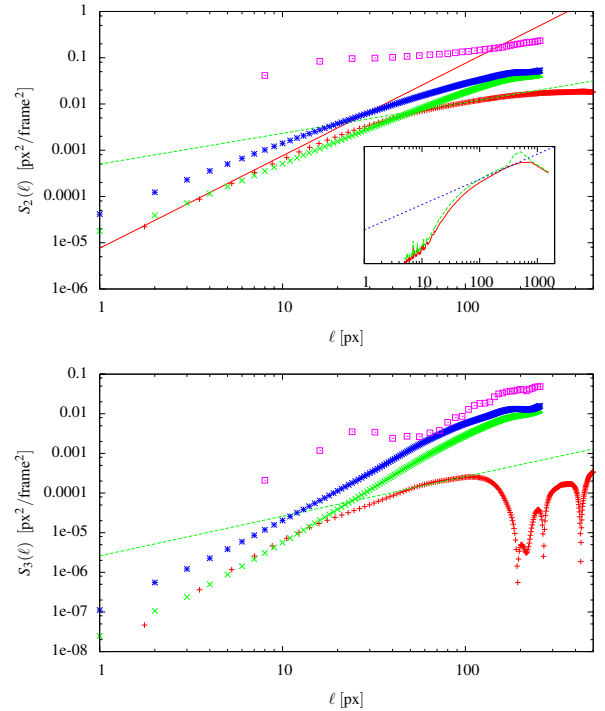

Figure 1: Comparisons of second-order (top) and third-order (bottom) longitudinal velocity structure functions in the streamwise direction for the wake flow (cylinder mounted horizontally). Red, HWA measurements; Green, proposed method; Blue, Horn & Schunck [5]; Purple, correlation method; Solid line is $\sim \ell^2$; Dash line is $\sim \ell^{(2/3)}$ on top and $\sim \ell$ on bottom. Energy spectra of the streamwise velocity is shown in inset.

Figure 1 and 2 show, for the wake flow, comparisons between the proposed multiscale method and HWA measurements of the second- and third-order longitudinal velocity structure functions $S_2(\ell)$ and $S_3(\ell)$ for various length scales in the streamwise

direction.The agreement between HWA and the present method is good up to 40 pixels for the wake flow with the cylinder mounted horizontally and 80 pixels with the cylinder mounted vertically. It reflects the fact that the small scales were estimated accurately. The deviation for larger separations is explained by the limit of validity of Taylor's hypothesis and the weak statistical convergence of $S_p(\ell)$.
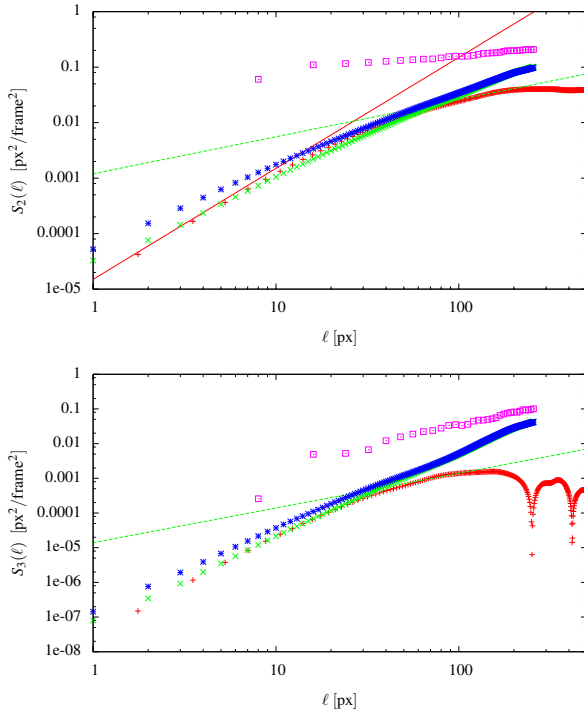

Figure 2: Wake flow (cylinder mounted vertically).See figure 2 for details.

The results obtained by Horn and Schunck [5] method and correlation technique is plotted for comparisons. The present approach (based on (6)) is superior because it accounts for the whole dynamic range involved in the flow, i.e. from the integral scale to the Kolmogorov dissipation scale.

This phenomenon is emphasized for the case of the grid turbulence for which the present method allows the estimation of small scale turbulence represented by vortices smaller than 10 pixels diameter (see figure 3) and velocity fluctuations as low as 0.02 pixels. For this case this led to the resolution of a dynamic range of 60 since the largest displacements were of the order of 1.2 pixels. It should be noted that for this flow with energy level sustained across the small scales, classical optical flow method ([5]) and correlation approach estimated only spurious vector fields.

6. CONCLUSIONS

In this work we have proposed a new physics-based multiscale PIV approach. The technique involves a regularization constraining the velocity fields, through the second order structure function, to follow the statistical scaling laws as predicted by Kolmogorov. The real parameters of the power-law, corresponding to the distribution of the turbulent kinetic energy decay, were estimated from a simple hot-wire measurement. Results showed the ability of the method to estimate in turbulent flows large dynamic ranges and better accuracy than other PIV methods.
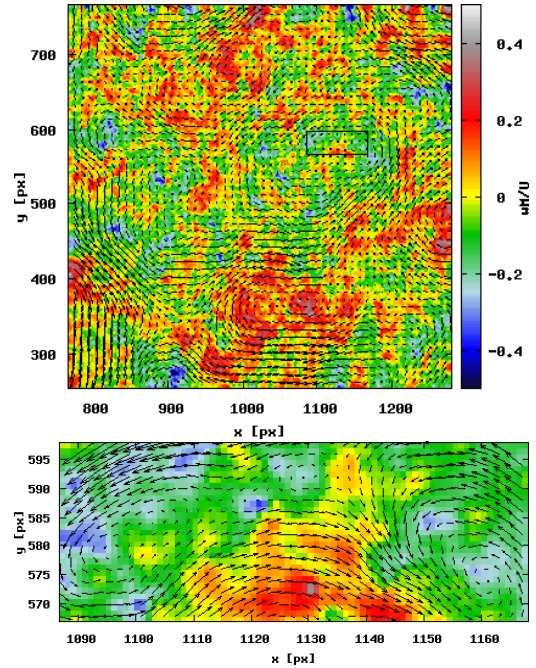

Figure 3: Velocity field and vorticity map estimated with the present self-similar regularization method for grid turbulence.

REFERENCES

[1] T. Corpetti, D. Heitz, G. Arroyo, E. Mémin, and A. Santa-Cruz. Fluid experimental flow estimation based on an optical-flow scheme. *Experiments in Fluids*, 40(1):80–97, 2006.

[2] U. Frisch. *Turbulence: the legacy of A.N. Kolmogorov.* Cambridge University Press, 1995.

[3] P. Héas, E. Mémin, D. Heitz, and P. Mininni. Turbulence power laws and inverse motion modeling in images. Technical report, INRIA, 2009.

[4] D. Heitz, P. Héas, E. Mémin, and J. Carlier. Dynamic consistent correlation-variational approach for robust optical flow estimation. *Experiments in Fluids*, 45(4):595–608, 2008.

[5] B.K.P. Horn and B.G. Schunck. Determining optical flow. *Artificial Intelligence*, 17:185–203, 1981.

[6] P. Lavoie, L. Djenidi, and A. Antonia. effects of initial conditions in decaying turbulence generated by passive grids. *Journal of Fluid Mechanics*, 585:395–420, 2007.

[7] T. Liu and L. Shen. Fluid flow and optical flow. *Journal of Fluid Mechanics*, 614:253–291, 2008.

[8] J. Yuan, C. Schnörr, and E. Mémin. Discrete orthogonal decomposition and variational fluid flow estimation. *Journal of Mathematical Imaging Vision*, 28:67–80, 2007.